Dyes and Pigments 244 (2026) 113096

Contents lists available at ScienceDirect

Dyes and Pigments

journal homepage: www.elsevier.com/locate/dyepig

Towards an easy production of novel pyoverdines by an antarctic *Pseudomonas* strain: a spectroscopic and HPLC-MS/MS characterization study

Marco Zannotti [a,e], Martina Di Sessa [a,b], Maria Chiara Biondini [b,c], Alberto Vassallo [c], Stefano Ferraro [a], Simone Angeloni [d], Massimo Ricciutelli [d], Sandra Pucciarelli [c,e,*], Rita Giovannetti [a,e,*]

[a] *Chemistry Interdisciplinary Project, School of Science and Technology, Chemistry Division, University of Camerino, 62032, Camerino, Italy*
[b] *University School for Advanced Studies IUSS Pavia, Pavia, 27100, Italy*
[c] *School of Biosciences and Veterinary Medicine, Biosciences and Biotechnology Division, University of Camerino, 62032, Camerino, Italy*
[d] *Chemistry Interdisciplinary Project, HPLC-MS Laboratory, University of Camerino, 62032, Camerino, Italy*
[e] *IridES S.r.l., Via Via Gentile III da Varano n° 1, 62032, Camerino, Italy*

A B S T R A C T

Bacterial secondary metabolites are fundamental molecules not only in several microbial processes, but also in various sectors of today's economy, especially in human health and agriculture. Siderophores are important secondary metabolites produced by various bacterial strains, including *Pseudomonas* species, under iron-deficient conditions. Pyoverdines are fluorescent types of siderophores with molecular mass between 889 and 1764 Da that have strong affinity to iron and other metals. In this study, *Pseudomonas* sp. ef1, isolated from a consortium associated with the Antarctic psychrophilic ciliate *Euplotes focardii*, was cultured under iron-deficiency conditions to induce pyoverdine production, in the presence of 1 % w/v glucose as a sole carbon source. The produced pyoverdines were purified and characterized by UV–Vis, fluorescence spectroscopy and HPLC-MS/MS analysis. The isolated and characterized compounds were represented by two different Group 1 Pyoverdines, both containing six amino acids peptide chain, with the following sequence: cOHOrn-Ala-Thr-Ala-OHAsp-Lys. The two pyoverdines differ only in the sidechain dicarboxylic acid, called R_{SC}, that usually consists either of succinic/malic acid or their monoamide analogues, or glutamic/α-ketoglutaric acid. One of the two pyoverdines produced by *Pseudomonas* sp. ef1 is reported for the first time. The study of novel pyoverdines contribute to understand the role of secondary metabolites in modulating bacterial consortia. Furthermore, it opens new perspective in different possible applications.

1. Introduction

Secondary metabolites produced by microorganisms has attracted considerable attention in recent years. Bacterial secondary metabolites are a major source of antibiotics and other bioactive compounds [1–3]. In microbial communities, these molecules can mediate interspecies interactions and responses to environmental change [4]. An important class of bio-compounds are siderophores, natural molecules that have a strong affinity to bind iron ion (formation constant $K_f > 10^{30}$ M^{-1}) [5–7], and different other metal ions. Iron is a key element for several cellular processes: it is involved in oxygen reduction for the ATP synthesis, in DNA replication and repair, oxygen transport, carbon metabolism [e.g., via the tricarboxylic acid (TCA) cycle] and regulation of gene expression [8,9]. Although iron is an abundant element, the reduced solubility of $Fe(OH)_3$, that prevails at neutral pH and in an oxidant environments, prevents its bioavailability [10,11]. Therefore, in response to the iron deficiency, microorganisms synthesize a class of natural compounds called siderophores. Several types of siderophores are naturally synthesized by bacteria and, depending on their chemical structure, they are categorized into catecholates and phenolates, hydroxamates, carboxylates, and mixed-type siderophores. Mixed-type siderophores, as pyoverdine, produced by *Pseudomonas* bacteria, contain two or even three siderophore classes simultaneously, such as a catecholate function and two hydroxamate functions, showing high-affinity for iron chelation [6,12,13]. PVDs are molecules in the range of molecular mass between 889 and 1764 Da [14] that shows fluorescent ability. PVD molecule is composed of three distinctive structural parts: i) a dihydroxyquinoline chromophore, responsible for its fluorescence, ii) a 6–12 amino acids peptide chain connected to the chromophore, and iii) a dicarboxylic acid, called sidechain (R_{SC}), that consists either of succinic/malic acid or their monoamide analogues, or glutamic/α-ketoglutaric acid. Several pyoverdines differ only for the

* Corresponding author. IridES S.r.l., Via Via Gentile III da Varano n° 1, 62032, Camerino, Italy.
E-mail addresses: marco.zannotti@unicam.it (M. Zannotti), sandra.pucciarelli@unicam.it (S. Pucciarelli), rita.giovannetti@unicam.it (R. Giovannetti).

https://doi.org/10.1016/j.dyepig.2025.113096
Received 27 February 2025; Received in revised form 31 July 2025; Accepted 3 August 2025
Available online 5 August 2025

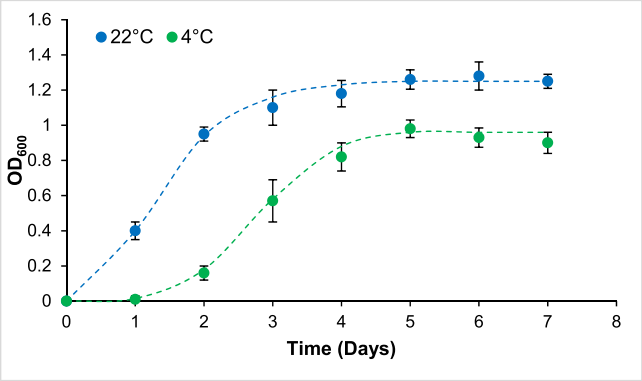

Fig. 1. Growth curves of *Pseudomonas* sp. ef1 in M9 medium supplemented with 1 % (w/v) of glucose at 4 °C (blue dash line) and 22 °C (blue line). The experimental data represents a mean ± standard deviation of three replicates.

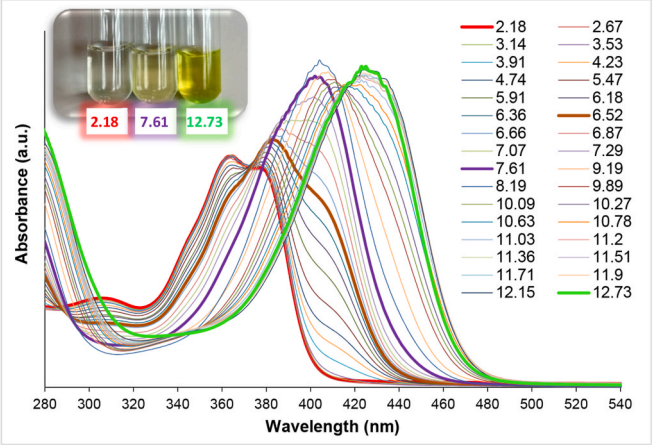

Fig. 2. UV–Vis spectral change of pyoverdine compounds in the pH range between 2.18 and 12.73; in the inset the colour variation of the pigment at acid, neutral and alkaline pH conditions.

acid moiety bound to the amino group [14–21]. Over 60 pyoverdines were reported and analysed in different studies [14,22].

Pyoverdines produced by fluorescent *Pseudomonas* species can be classified into four groups based on the structural properties of their peptide chains. In Group 1, the most prevalent pyoverdines possess a linear peptide chain terminating with cyclo-*N*-hydroxyornithine; some variants feature a tetrahydropyrimidine ring resulting from the condensation of diaminobutyric acid (Dab) with the preceding amino acid. Group 2 is characterized by a peptide chain with a C-terminal cyclic structure comprising three to four amino acids, formed through an amide bond between the terminal amino acid and an in-chain lysine.

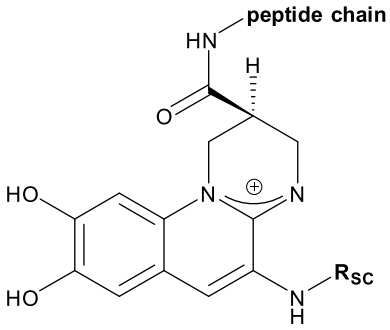

Fig. 3. Typical structure of Pyoverdine.

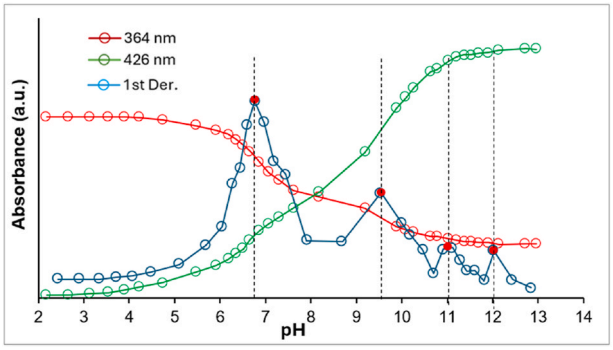

Fig. 4. Absorbance changes at 364 and 426 nm, and 1st derivative calculation at different pHs.

Group 3 includes a minority of pyoverdines whose peptide chains end with a C-terminal cyclodepsipeptidic substructure, produced by an ester bond between the terminal amino acid and an internal serine or threonine. Group 4 is distinguished by a free C-terminal carboxyl group, typically representing hydrolysis products of Group 3 cyclic esters, which are readily hydrolysed at pH levels of 9 or higher [23,24].

PVD molecules can be used in different fields of applications from medicines to agriculture [12].

Being a virulence factor, PVD is a promising target to detect pathogens and can be used to protect plants from infections [25]. Furthermore, PVDs can provide nutrients to plants, triggering selectively the mobilization of specific metal ions, for example by increasing the bioavailability of nickel respect of cadmium in hydroponics [8,26]. The ability to bind metal by PVDs can be exploited for bioremediation by removing iron from asbestos fibres or efficiently removing iron from chrysotile-gypsum and amosite-gypsum, as examples [27,28]. Finally, PVDs can form strong and stable complexes with actinides metals like U, *Cm* and Np, showing strong chelator ability [29]. The fluorescence behaviour can be also used for their use in sensor applications for the detection of metals and organic compounds [30,31].

For the characterization of PVD compounds and their congeners, they are analysed using tandem mass spectrometry (MS/MS) that shows the highest level of confidence, and by interpretating the fragmentation of the pseudo-molecular target ion, $[M+2H]^{2+}$, that commonly is the most abundant. In the double charged ion $[M+2H]^{2+}$, one proton is reasonably located on the chromophore due to its ability to delocalize the positive charge; the second proton, according to the "mobile proton" model, can be present on the different amide groups in the peptide chain favouring the cleavages in the near vicinity, giving useful information about the amino acid sequence of the pyoverdine structure [5,7,14,17,18,21,22,32–36].

In this study, the ability of the Antarctic bacteria *Pseudomonas* sp. ef1, isolated from a consortium associated to the Antarctic psychrophilic *Euplotes focardii* [37–39] to biosynthesize pyoverdines under iron-deficient conditions, using 1 % w/v glucose as the sole carbon source, has been reported. The produced PVD compounds were deeply characterized by UV–Vis, fluorescence spectroscopy and by HPLC-MS/MS and the structure of two different PVDs has been identified, one of these never reported before.

2. Experimental section

2.1. Bacterial culture, growth conditions and pyoverdine production

The bacterial strain reported in this work was isolated from a consortium associated with the Antarctic psychrophilic ciliate *E. focardii* and named as *Pseudomonas* sp. ef1. After isolation, the strain was stored at −80 °C in glycerol stock and spread on LB agar plates (10 g/L Tryptone, 5 g/L yeast extract, 5 g/L NaCl, 15 g/L bacto-agar) and let grown at

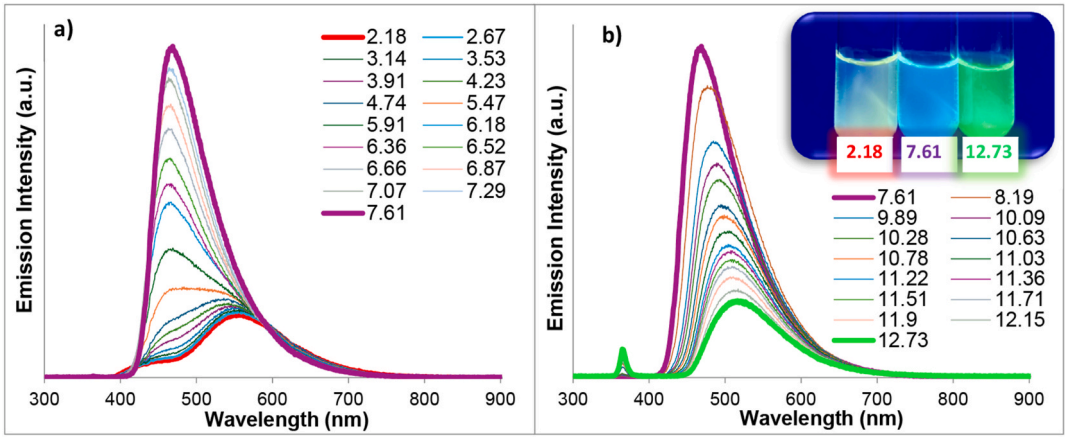

Fig. 5. Emission spectra of the pigment (Excitation = 365 nm) at different pH values: a)2.17–7.61 and b) 7.61–12.73.

21 °C. For pyoverdine production, the bacterial cells from the overnight-grown culture were inoculated in 500 mL of M9 medium, supplemented with 1 % w/v glucose as a sole carbon source, and incubated at 21 °C in a 2 L-Erlenmeyer flask under shaking (180 rpm). Composition of M9 medium is as follows: Na_2HPO_4 6 g/L, KH_2PO_4 3 g/L, NaCl 0.5 g/L, NH_4Cl 1 g/L, $MgSO_4$ 2 mM, $CaCl_2$ 0.1 mM. Solutions of $MgSO_4$, $CaCl_2$ and glucose (1 %w/v) were separately sterilized by autoclave and added just before use. The pH was adjusted to 7.4 with NaOH before sterilization. The bacterial growth was monitored by measuring the optical density at 600 nm (OD600) using a NanoDrop (Thermo Scientific™) spectrophotometer. Three replicates for each test were measured. In addition, the growth of the bacteria at 21 °C was also monitored in presence of $FeCl_3$ salt in M9 agar plates supplemented with 1 % glucose. All the media, reagents and salts used were provided by Merck (Milan, Italy) and used without further purification.

2.2. Sample preparation and UV–Vis characterization

The bacterial culture was centrifuged at 8000×*g* for 10 min at room temperature and the supernatant was filtrated by PTFE sterile ReliaPrep Syringe™ filters (0.22 mm, Ahlstrom) to completely remove bacterial cells from samples to obtain a water solution containing the yellow pigment.

SPE purification was performed using a Strata-XL 100 μm polymeric reversed-phase column (Phenomenex, Torrance, CA, USA) to purify the sample and remove excess salts by selectively eluting only the fluorescent fraction.

The SPE column was initially conditioned with methanol 1 mL with a successive equilibration with 1 ml of ultrapure water. The sample was then loaded (1 mL) and washed two times with water (2 × 300 μL). The elution was finally made using H_2O/MeOH(70/30) + 0.1 % of formic

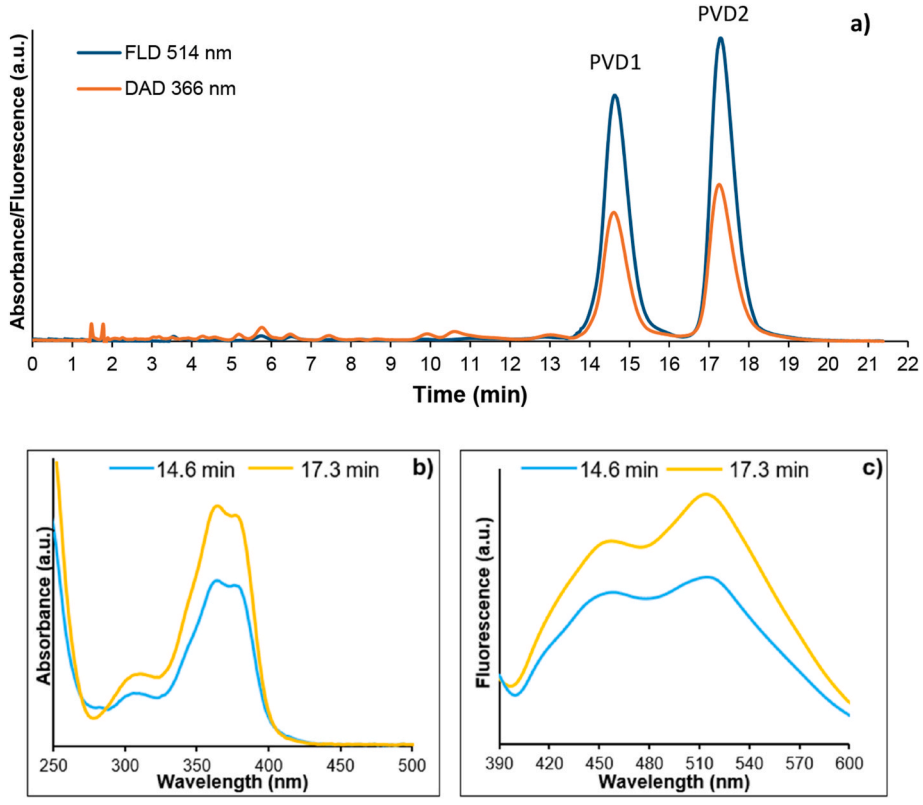

Fig. 6. a) HPLC-DAD-FLD chromatogram, by isocratic elution H_2O/MeOH (90/10) with formic acid 0.1 %, of the pigment and the relative b) UV-VIS and (c) emission spectra of the PVDs eluted at 14.6 and 17.3 min.

acid (2 × 300 μL).

The yellow pigment was then characterized by UV–Vis spectroscopy using an Agilent 8454 Cary UV–Visible Diode Array Spectrophotometer (Agilent, Santa Clara, USA). The UV–Vis spectral change at different pH was monitored by micro-additions of HCl and NaOH 1 M (Carlo Erba reagents, Cornaredo, MI, Italy). The emission spectrum of the samples was monitored using an Ocean HDX Fluorimeter (Ocean Insight), equipped with a monochromatic laser at 365 nm.

2.3. Liquid chromatography and mass-spectrometry analysis

The yellow pigment was analysed by HPLC 1260 Infinity (Agilent, Santa Clara, USA) equipped with a diode Array (DAD) and fluorescent (FLD) detectors. The separation was performed using an isocratic elution, the mobile phase was composed by water (A, 90 %) and methanol (B, 10 %), both with formic acid 0.1 % with a flow rate of 1 mL/min. The analysis was achieved using a C18 Kinetex (250 × 4.60 mm, particles size 5 μm) from Phenomenex (Torrance, CA, USA). The injection volume was 5 μL; the temperature of the column was set at 30 °C. The monitored wavelengths were 306, 364, 377 nm using DAD, while for FL, the wavelengths monitored were 464, 514, 555 nm (excitation 365 nm).

HPLC-MS/MS analysis were performed using an HPLC Agilent 1290 Infinity coupled with a Triple Quadrupole 6420 (Agilent, Santa Clara, USA) with an electrospray (ESI) source operating in positive mode. The column and the operative conditions of the separation were the same used for HPLC-DAD-FLD analysis. The source parameters were set as follow: the temperature of the drying gas was 350 °C; the gas flow was 12 L/min^{-1}; the nebulizer pressure was 55 psi; and the capillary voltage was 4000 V. The acquisitions were performed in scan mode and once identified some interesting precursor ions the acquisitions were carried out in product ion scan mode. For each selected precursor ion, the fragmentation of the investigated compounds was monitored at different collision energy: 16, 30 and 40 eV.

For all the analysis, the sample was filtered through a 0.2 μm single use syringe filter from Phenomenex (Bologna, Italy).

3. Results and discussions

3.1. Pseudomonas sp. ef1 growth and pyoverdine production

The bacterial growth of the *Pseudomonas* sp. ef1 in M9 supplemented with 1 % w/v glucose as sole carbon source has been monitored at 4 °C and 22 °C, that represent respectively the ideal growing temperature of the Antarctic *E. focardii* ciliate host [39] and that of the isolated *Pseudomonas* sp. ef1 [40]. In Fig. 1, the optical density at 600 nm (OD_{600}) is reported as function of time: *Pseudomonas* can growth in this medium at both 4 °C and 22 °C, but at 22 °C the bacterial culture reaches the plateau earlier than at 4 °C. At both temperatures, the culture becomes fluorescent once reached the plateau. The fluorescent bioproduct was purified as described under Material and Methods for further analysis.

Pseudomonas sp. ef1 growth was also estimated at 22 °C in M9 agar plates supplemented with 1 % glucose in the presence or absence of $FeCl_3$, demonstrating that, in the presence of iron, the cultures are not fluorescent (Fig. S1), suggesting that the bioproduct is a siderophore.

3.2. Spectroscopic characterization of the fluorescent pigment

The bacterial fluorescent pigment was characterized by UV–Vis spectroscopy at different pH values (Fig. 2). At pH 2.18, the colour of the pigment solution was pale-yellow, almost transparent, and the spectrum shows two mainly bands at 364 and 378 nm. Increasing the pH, the absorption band at 364 nm started to decrease, while the band at 378 nm increased and red-shifted to higher wavelength; in addition, a new absorption band at 406 nm started to increase after pH 3.53. At pH 7.61, the band at 364 completely disappeared and, towards alkaline pH, the band at 406 nm increase up to a pH about 8.19; after this value, the band at 406 nm decrease and red shift-shifted to 426 nm, as broadened band at pH of 12.73. At alkaline pH the sample shows an intense green-yellow colour as reported in the inset of Fig. 2. The observed UV–Vis spectral behaviour is consistent with the presence of pyoverdine compounds in the solution [41–43].

Typical structure of pyoverdine is reported in Fig. 3, where the dihydroxyquinoline chromophore, responsible for the fluorescence, is directly linked by amide bond to the peptide chain sequence, that consists of 6–12 amino acids, and to a dicarboxylic acid side chain (R_{SC}), that usually consist of succinic/malic acid or the monoamide analogues, or glutamic/α-ketoglutaric acid [14–21].

As first described by Albrecht-Garry et al. [42], the spectral changes reported in Fig. 3, which correspond to pH variations, can be correlated with the first and second deprotonation of the –OH groups in the dihydroxyquinoline chromophore, as well as with the acid-base properties of the R_{SC} moieties present in the pyoverdine structure.

The spectral changes, corresponding to the pH variation, can be correlated to the first and the second deprotonation of the –OH groups of the di-hydroxyquinoline chromophore, and about the R_{SC} moieties acid-base features, present in the pyoverdine's structure, as reported in Fig. 3. Analysing the absorbance of the characteristic wavelengths at 364 nm and 426 nm as function of the pH (Fig. 4), an estimation of the pK_as values can be calculated from the first derivative of the data, associated to the flex points, as it is possible to observe in the plot of Fig. 4. From the calculation of the first derivative four pK_as values have been find.

The pK_{a1} at around 6.7 can be attributable to the first –OH group (pK_{a1}) on the dihydroxiquinoline structure and about 11 for the second –OH (pK_{a3}) [37–39]. An additional pK_a can be estimated from the absorption profile and it was detected at around pH 9.5 (pK_{a2}); this can be due to the presence of an amino group in the vicinity of the chromophore that influence its absorption behaviour.

An additional maximum peak has been calculated at pH 12; in that case can be traced to the deprotonation of an additional –OH group on the R_{SC} side chain (pK_{a4}), as example for the presence of hydroxy succinic amide, that is an R_{SC} reported as pyoverdine dicarboxylic side chain in pyoverdine compounds produced by *Pseudomonas* sp. ef1.

The emission spectra have been also investigated at different pH values and the obtained fluorescence spectra are reported in Fig. 5. The emission behaviour depends on the pyoverdine's form. In fact, at acidic pH in water solutions, the protonated form of pyoverdine shows a typical emission peak centred at 554 nm of lower intensity, while, increasing the pH, the emission intensity strongly increases and blue-shifts to 466 nm; the maximum emission intensity was detected for the pH 7.6. After the last reported value, a further increase in pH leads to a decrease of the emission intensity that red-shift to 520 nm for the strongest alkaline pyoverdine's solution at pH 12.73.

3.3. Characterization by HPLC-DAD-FLD analysis

Since it is known that these bacteria generally do not produce a single pyoverdine molecule but instead a group of different pyoverdines [5,14], to verify the number and types of pyoverdines produced by *Pseudomonas* sp. ef1, HPLC analysis with DAD and FLD detectors has been performed to analyse the yellow pigment.

In Fig. 6a are reported the superimposed HPLC DAD/FLD chromatograms by using H_2O/MeOH (90/10), both with formic acid 0.1 % as the mobile phase. The results confirm the presence of two strong peaks with high fluorescence that eluted at 14.6 and 17.3 min.

In Fig. 6b and c are reported the UV–Vis and fluorescence spectra that are consistent with different pyoverdines compounds in acidic pH.

3.4. Characterization by HPLC-MS/MS analysis

To detect and characterize the different PVDs and evaluate their respective molecular weights, these have been analysed by HPLC-MS

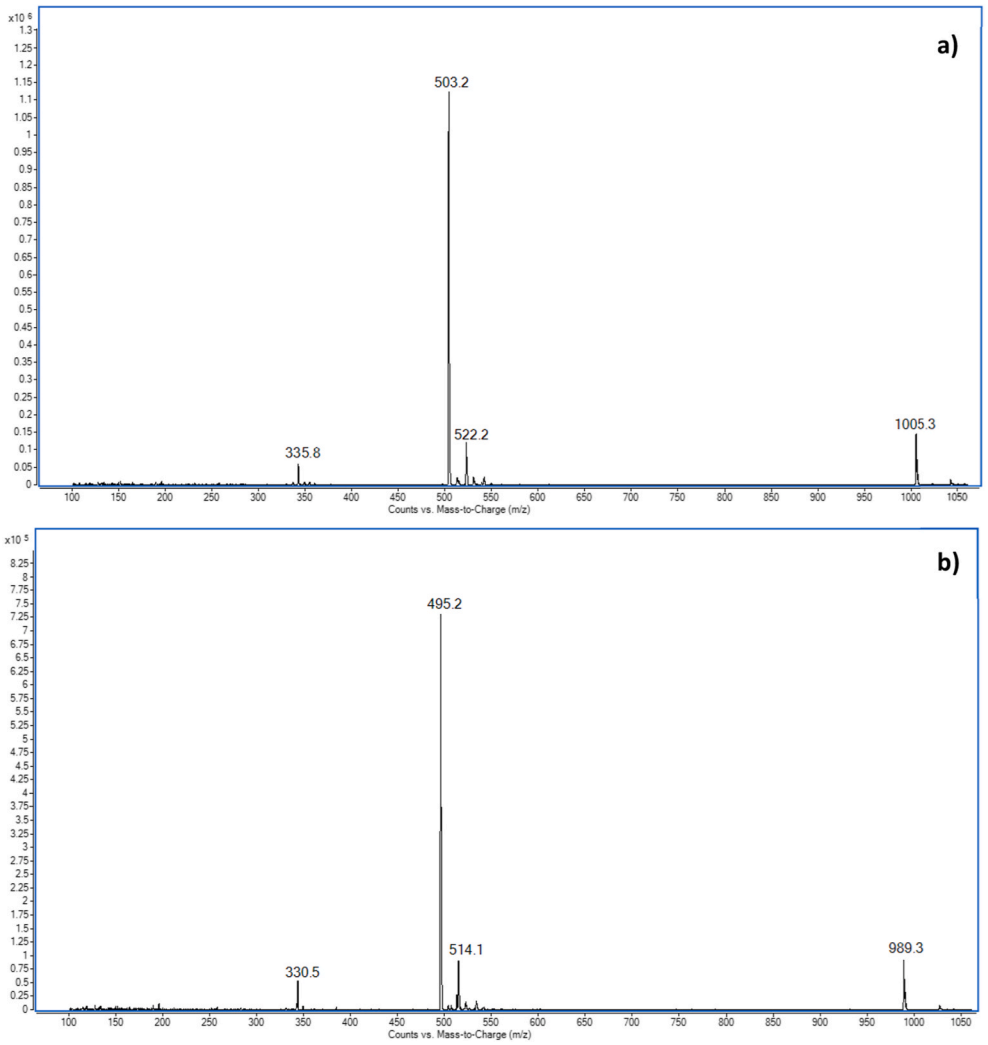

Fig. 7. MS-spectrum of the PVDs detected at a) 14.3 and b) 17.3 min by HPLC-MS analysis.

and tandem HPLC-MS/MS by using the same analytical protocol. The total ion current chromatogram (TIC) reported in Fig. S2 shows two main distinct peaks at around 14.6 min and 17.3 min corresponding to the retention times of the analytes under investigation.

Analyzing the MS-spectrum of the two peaks investigated, reported in Fig. 7a and b, for both the compounds, four characteristic ion species have been detected: the pseudo-molecular ion $[M+H]^+$ at *m/z* 1005.3 and 989.3, for PVD1 and PVD2 respectively, the double and triple charged ions $[M+2H]^{2+}$ and $[M+3H]^{3+}$ and, in addition, the adduct with potassium $[M + H + K]^{2+}$. All the results obtained from HPLC-MS analysis in scan mode are reported in Table 1.

Fig. 8 reports the extracted ion chromatograms (EIC) of the two most abundant adduct ions $[M+2H]^{2+}$ at *m/z* 503.2, and 495.2 for the two distinctive PVDs compounds confirming that the reported *m/z* ions are specific of the two selected peaks at 14.6 and 17.3 min.

Successively, the $[M+2H]^{2+}$ ions of the two PVD molecules have been fragmented using various collision energies, in order to confirms the presence of the characteristic fragments and to have information about the amino acid sequence [17–19,22,23,30–34].

In Figs. 9 and 10 are reported the MS/MS spectrum of the PVD1 and PVD2 at 16 and 40 eV, respectively.

The ion $[M+2H]^{2+}$ is typically used as a precursor for the fragmentation due to its higher abundance with respect the monocharged ion $[M+H]^+$ (Fig. 7); in addition, in the double charged ion, the second proton, following the mobile proton scheme, can lies at the different peptide bonds and promote the cleavage of the peptide chain, giving the information about the amino acids sequence [17]. The fragmentation scheme is reported in Figs. 9 and 10.

For both the compounds, in the MS/MS spectra (Figs. 9a–10a), at

Table 1
Molecular mass and the related *m/z* corresponding to the different PVDs.

PVD	$[M+3H]^{3+}$	$[M + H + K]^{2+}$	$[M+2H]^{2+}$	$[M+H]^+$	M
1	335.8	522.2	503.2	1005.3	1004.3
2	330.5	514.1	495.2	989.3	988.3

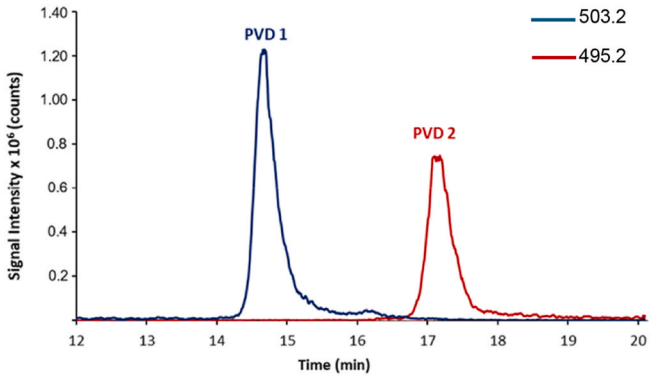

Fig. 8. Extracted ion chromatograms (EIC) of the pigment produced by *Pseudomonas* sp. ef1.

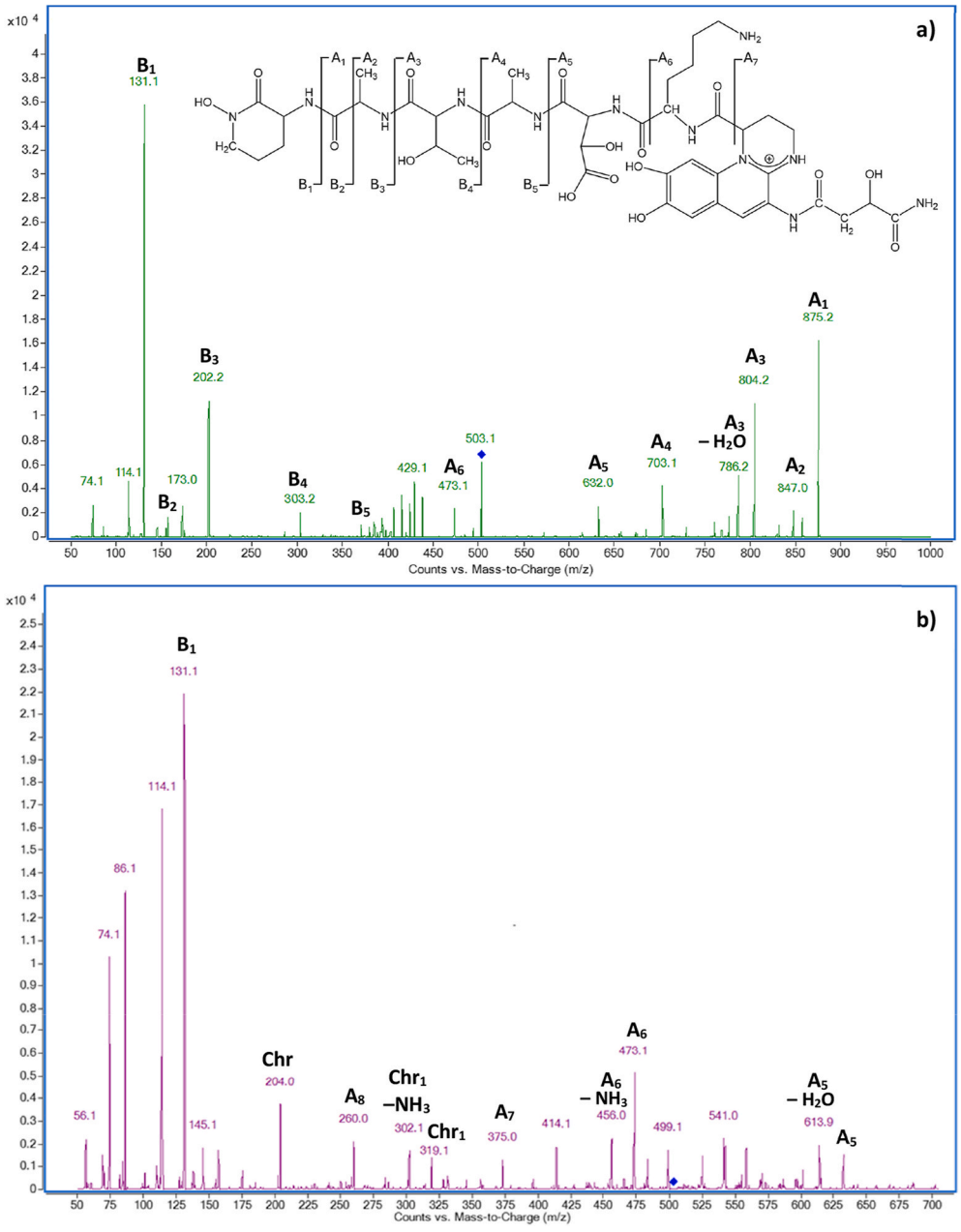

Fig. 9. MS/MS spectra of the $[M+2H]^{2+}$ (*m/z* 503.1) at a) 16 and b) 40 eV of collision energy. In the inset of a) reported the fragmentation scheme.

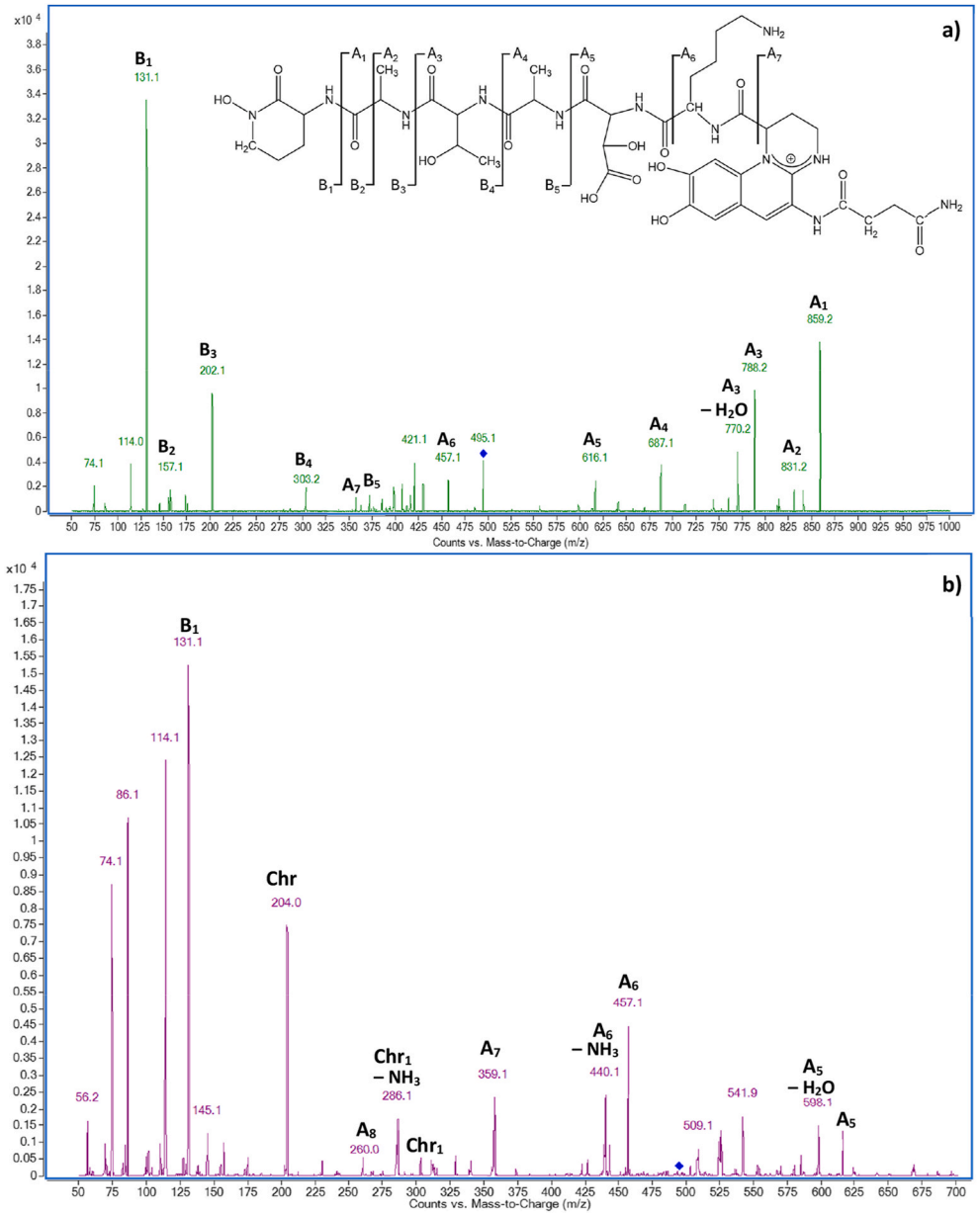

Fig. 10. MS/MS spectra of the $[M+2H]^{2+}$ (*m/z* 495.1) at a) 16 and b) 40 eV of collision energy. In the inset of a) is reported the fragmentation scheme.

Table 2
Ion fragments detected by HPLC-MS/MS of the PVD1 and PVD2 and the relative *m/z* signals.

Fragments	Ion/Ion fragments	PVD 2 *m/z*	PVD 1 *m/z*
$[M+H]^+$	[cOHOrn-Ala-Thr-Ala-OHAsp-Lys-Chr–NH–R_{sc} + H]$^+$	989.3	1005.3
A_1	[M − cOHOrn + H]$^+$	859.2	875.2
A_2	[M − B_2 + H]$^+$	831.2	847.0
A_3	[M − cOHOrn – Ala + H]$^+$	788.2	804.2
$A_3 – H_2O$	[$A_3 – H_2O$]$^+$	770.2	786.2
A_4	[M − cOHOrn – Ala– Thr + H]$^+$	687.1	703.1
A_5	[M − cOHOrn – Ala-Thr-Ala + H]$^+$	616.1	632.0
$A_5 – H_2O$	[$A_5 – H_2O$]$^+$	598.1	613.9
A_6	[Lys-Chr–NH–Rsc + H]$^+$	457.1	473.1
$A_6 – NH_3$	[$A_6 – NH_3$]$^+$	440.1	456.0
A_7	[Chr–NH–R_{sc} + H]$^+$	359.1	375.0
A_8	[Chr-NH_2 + H]$^+$	260.0	260.0
Chr_1	After RDA from A_6	303.1	319.1
$Chr_1 – NH_3$	[$Chr_1 – NH_3$ + H]$^+$	286.1	302.1
Chr	[$Chr_1 – R_{sc}$ + H]$^+$	204.0	204.0
B_1	[cOHOrn + H]$^+$	131.1	131.1
B_2	[cOHOrn-COH + H]$^+$	157.1	157.1
B_3	[cOHOrn-Ala + H]$^+$	202.1	202.1
B_4	[cOHOrn-Ala-Thr + H]$^+$	303.2	303.2
B_5	[cOHOrn-Ala-Thr-Ala + H]$^+$	374.2	374.2

lower *m/z* value, high-intensity signals at *m/z* 131.1, accompanied by a lower *m/z* signal at 114, have been detected; these fragments signals are relative to the terminal *N*-hydroxyl(cyclo)Ornithine (cOHOrn), that is the last amino acid on the peptide chain, indicated as B_1. This confirms that both PVDs belong to Group 1.

All the fragments detected by HPLC-MS/MS relative to the PVD1 and PVD2 following the fragmentation scheme showed in Figs. 9 and 10, are reported in Table 2.

At higher collision energy (40eV) for both the PVDs (Figs. 9b–10b), high intensity peak of the fragment ions at *m/z* 86.1, 114.1 and 131.1 for the terminal cOHOrn has been always detected.

In addition, at high collision energy, the fragments A_6, that corresponds to the chromophore bind to the L-Lysine and the R_{SC} moiety, can be clearly detected at 473.1and 457.1 *m/z*, for PVD1 and PVD2, respectively. In Scheme 1 is reported the fragmentation pattern starting from the ion fragment A_6 with the related ions and *m/z*. The fragment A_7, relative to the loss of the L-lysine from A_6 are detected at 375.1 and 359.1 *m/z*, for PVD 1 and PVD 2, respectively. Therefore, in this study, the only difference between the two pyoverdine produced by *Pseudomonas* sp. ef1 is due to the different R_{SC} moieties bind to the chromophore, that for PVD1 is the hydroxy succinic acid amide and, for the PVD2, is the succinic acid amide, as reported in Scheme 1. The fragment ions related to chromophore after the loss of the dicarboxylic side chain (R_{SC}) at *m/z* 260.0 (Scheme 1) can be also detected for both PVD1 and PVD2 at 40eV, as reported in the MS/MS spectra (Figs. 9b–10b) [18].

The fundamental fragment ion at *m/z* 204.0 (Chr), that corresponds to the characteristic 2-3-diamino-6,7-dihydroxyquinoline chromophore of the pyoverdine [7,17,22,32] and confirms its presence, has been not detected at low collision energy (16eV), but for both the compounds is identified at high collision energy at 40eV. This ion species arises from the retro Diels-Alder reaction of the chromophore, reported in Scheme 2, where R_{SC} is relative to the dicarboxylic side chain. The intermediate fragment ions (Chr_1), relative to the dihydroxyquinoline chromophore bind to the R_{SC} side chain, can be detected at 319.1 and 303.1 *m/z* for PVD1 and PVD2, respectively, with the corresponding fragment ions at *m/z* 286.1 and 302.1 relative to the ions after the loss of NH_3 (Figs. 9b–10b).

These fragmentation pattern has been also confirmed by the precursor ion scan chromatogram, reported in Fig. 11, showing that the *m/z* fragments at 204.0 and 260.0 (set as product ions in the precursor ion scan acquisitions) are in common between the two pyoverdines; in this case the precursor ion scan chromatogram also include the *m/z* 131.1 of the terminal cOHOrn amino acid.

In addition, analyzing the peak at *m/z* 202.1 and 204.0, relative to the B_3 fragment ions and to the chromophore (Chr), it is interesting to observe their intensity ratio evolution as function of the collision energies, as reported in Fig. 12. At three different collision energies 16, 30 and 40eV, at lower energy the ion at *m/z* 202.1 (B_3) is the predominant while, increasing the energy, the ion relative to the chromophore is the predominant, confirming the presence of the dihydroxyquinoline chromophore, indicating that, for the detection of pyoverdine chromophore using ESI-MS/MS, it is necessary to operate at higher collision energies.

In conclusion, the Antarctic bacteria *Pseudomonas* sp. ef1 biosynthesized two different pyoverdines composed of the same peptide chain sequence of six amino acids*:* cOHOrn-Ala-Thr-Ala-OHAsp-Lys, with the cOHOrn as terminal amino acid. The two PVDs differs only in the R_{SC} moiety bind to the chromophore, that for PVD1 is the hydroxy succinic acid amide and, for the PVD2, is the succinic acid amide. Specifically the PVD1, is characterized for the first time, no evidence it is reported in literature, as is possible to observe in Table 3, that reports

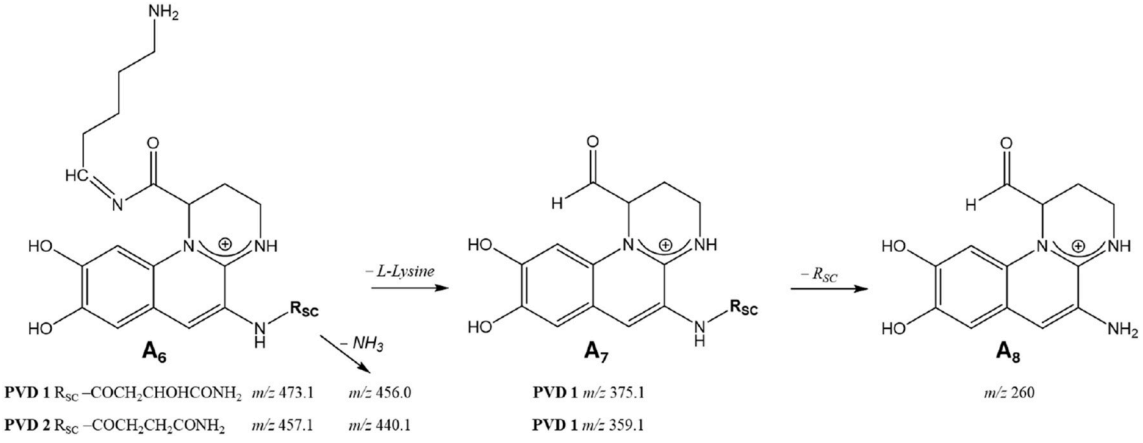

Scheme 1. Fragmentation of the A_6 ions and the formation of the ions A_8 at *m/z* 260.0.

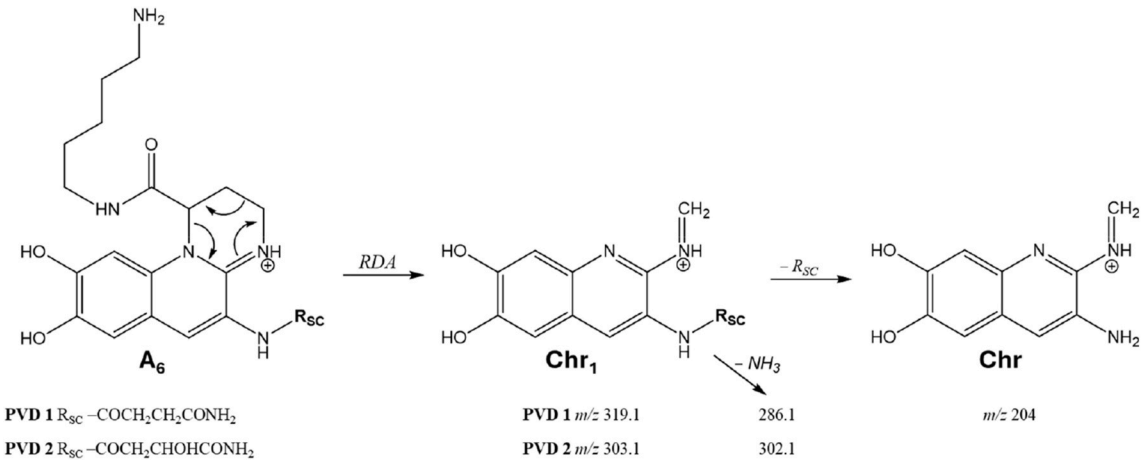

Scheme 2. Fragmentation of the pyoverdine chromophore by Retro-Diels Alder reaction.

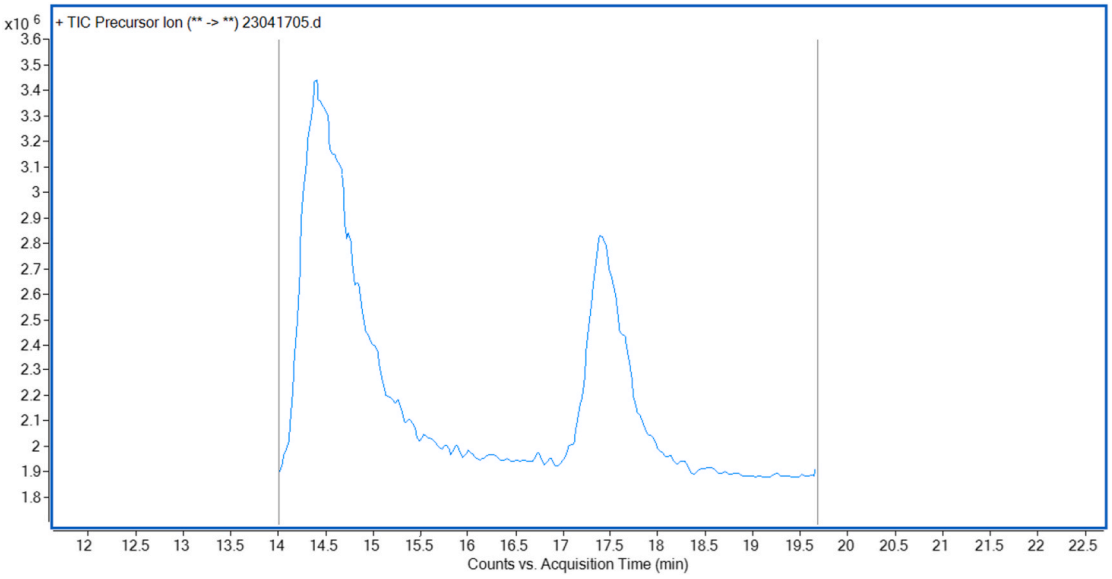

Fig. 11. Precursor ion chromatogram for the *m/z* precursor ions at 131.1, 204.0 and 260.0.

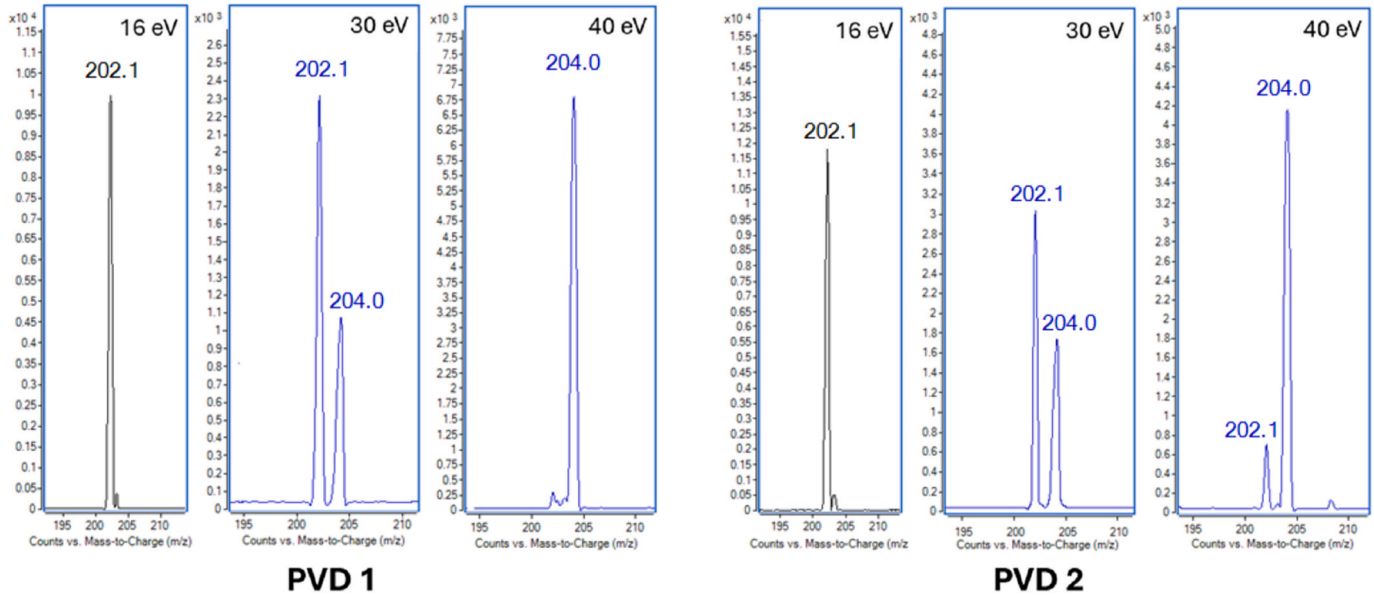

Fig. 12. MS/MS spectra of PVD1 and PVD2 at different collision energies (16, 30 and 40eV).

Table 3
Group 1 pyoverdines, characterized by a six-amino-acid peptide chain, biosynthesized by different *Pseudomonas* bacteria reported in literature.

Peptide chain sequence	$[M+H]^+$	R_{SC}	REFERENCES
Lys-OHAsp-Ala-Thr-Ala-cOHOrn	989	Succinic acid amide	[5,44]
Lys-OHAsp-Ser-Ser-Ser-cOHOrn	1007	Succinic acid amide	[14]
Ser-Lys-OHHis-Thr-Ser-cOHOrn	1043	Hydroxy succinic acid amide	[45]
Ala-Lys-Thr-Ser-AcOHOrn-cOHOrn	1046	Succinic acid	[5,46]
Asp-Ala-Asp-AcOHOrn-Ser-cOHOrn	1047	Succinic acid	[5,47]
Lys-OHAsp-Ala-Thr-Ala-cOHOrn	989.3	Succinic acid amide	This study
Lys-OHAsp-Ala-Thr-Ala-cOHOrn	**1005.3**	**Hydroxy succinic acid amide**	**This study (NEW)**

R_{SC}: dicarboxylic side chain.

the PVDs produced by different *Pseudomonas* bacteria with peptide chain sequence of six amino acids.

4. Conclusions

In this study, a yellow, fluorescent pigment produced by an Antarctic *Pseudomonas* sp. ef1 in the presence of only glucose as carbon source was purified and subsequently characterized. The obtained pigment showed absorbance and fluorescence profiles typical of pyoverdine compounds. For its characterization, an analytical method using HPLC-DAD-FLD and HPLC-MS/MS was developed. The analysis demonstrated that the pigment is a mixture of two Group 1 PVDs composed by the following sequence of six amino acids: cOHOrn-Ala-Thr-Ala-OHAsp-Lys.

The two PVDs differ to each other only in the R_{SC} moiety, and one of these is characterized for the first time. This implies that the Antarctic bacterium *Pseudomonas* sp. ef1 is as source of a novel PVD characterized for the first time in this work.

Microbial communities influence the health of every ecosystem on Earth, including humans. Microbes have a role in biogeochemical cycles and to determine the difference between host health and disease. Microbiomes are often highly complex, in part due to their biodiversity and metabolic responses that they display. The discovery of novel secondary metabolites, especially from a bacterial strain associated with an Antarctic consortium, may provide new insight in understanding their role in mediating microbial interactions and mechanisms of environmental adaptation.

CRediT authorship contribution statement

Marco Zannotti: Writing – review & editing, Writing – original draft, Validation, Supervision, Software, Methodology, Investigation, Data curation, Conceptualization. **Martina Di Sessa:** Validation, Investigation, Formal analysis, Data curation. **Maria Chiara Biondini:** Validation, Investigation, Formal analysis, Data curation. **Alberto Vassallo:** Validation, Investigation, Formal analysis, Data curation. **Stefano Ferraro:** Validation, Supervision, Software, Methodology, Investigation, Formal analysis, Data curation. **Simone Angeloni:** Software, Investigation, Formal analysis, Data curation. **Massimo Ricciutelli:** Software, Investigation, Formal analysis, Data curation. **Sandra Pucciarelli:** Writing – review & editing, Validation, Supervision, Methodology, Investigation, Data curation, Conceptualization. **Rita Giovannetti:** Writing – review & editing, Writing – original draft, Visualization, Supervision, Project administration, Methodology, Investigation, Data curation, Conceptualization.

Declaration of competing interest

The authors declare that they have no known competing financial interests or personal relationships that could have appeared to influence the work reported in this paper.

Acknowledgements

This paper and related research have been conducted during and with the support of the Italian national inter-university PhD course in Sustainable Development and Climate change (link: www.phd-sdc.it).

Appendix A. Supplementary data

Supplementary data to this article can be found online at https://doi.org/10.1016/j.dyepig.2025.113096.

Data availability

Data will be made available on request.

References

[1] Ramírez-Rendon D, Passari AK, Ruiz-Villafán B, Rodríguez-Sanoja R, Sánchez S, Demain AL. Impact of novel microbial secondary metabolites on the pharma industry. Appl Microbiol Biotechnol 2022;106(5–6):1855–78. https://doi.org/10.1007/s00253-022-11821-5.
[2] Newman DJ, Cragg GM. Natural products as sources of new drugs from 1981 to 2014. J Nat Prod 2016;79(3):629–61. https://doi.org/10.1021/acs.jnatprod.5b01055.
[3] Vollenweider V, Roncoroni F, Kümmerli R. Pyoverdine–antibiotic combination treatment: its efficacy and effects on resistance evolution in Escherichia coli. microLife 2024;5:uqae021. https://doi.org/10.1093/femsml/uqae021.
[4] Chevrette MG, Thomas CS, Hurley A, Rosario-Mélendez N, Sankaran K, Tu YX, Hall A, Magesh S, Handelsman J. Microbiome composition modulates secondary metabolism in a multispecies bacterial community. P Natl Acad Sci USA 2022;119(42):e2212930119. https://doi.org/10.1073/pnas.2212930119.
[5] Rehm K, Vollenweider V, Kümmerli R, Bigler L. Rapid identification of pyoverdines of fluorescent spp. by UHPLC-IM-MS. Biometals 2023;36(1):19–34. https://doi.org/10.1007/s10534-022-00454-w.
[6] Hider RC, Kong XL. Chemistry and biology of siderophores. Nat Prod Rep 2010;27(5):637–57. https://doi.org/10.1039/b906679a.
[7] Rehm K, Vollenweider V, Kümmerli R, Bigler L. A comprehensive method to elucidate pyoverdines produced by fluorescent pseudomonas spp. by UHPLC-HR-MS/MS. Anal Bioanal Chem 2022;414(8):2671–85. https://doi.org/10.1007/s00216-022-03907-w.
[8] Dell'Anno F, Vitale GA, Buonocore C, Vitale L, Esposito FP, Coppola D, Della Sala G, Tedesco P, de Pascale D. Novel insights on pyoverdine: from biosynthesis to biotechnological application. Int J Mol Sci 2022;23(19):11507. https://doi.org/10.3390/ijms231911507.
[9] Swayambhu G, Bruno M, Gulick AM, Pfeifer BA. Siderophore natural products as pharmaceutical agents. Curr Opin Biotech 2021;69:242–51. https://doi.org/10.1016/j.copbio.2021.01.021.
[10] Cézard C, Farvacques N, Sonnet P. Chemistry and biology of pyoverdines, primary siderophores. Curr Med Chem 2015;22(2):165–86. https://doi.org/10.2174/0929867321666141011194624.
[11] Nadal-Jimenez P, Koch G, Reis CR, Muntendam R, Raj H, Jeronimus-Stratingh CM, Cool RH, Quax WJ. PvdP is a tyrosinase that drives maturation of the pyoverdine chromophore in Pseudomonas aeruginosa. J Bacteriol 2014;196(14):2681–90. https://doi.org/10.1128/Jb.01376-13.
[12] Saha M, Sarkar S, Sarkar B, Sharma BK, Bhattacharjee S, Tribedi P. Microbial siderophores and their potential applications: a review. Environ Sci Pollut Res 2016;23(5):3984–99. https://doi.org/10.1007/s11356-015-4294-0.
[13] Timofeeva AM, Galyamova MR, Sedykh SE. Bacterial siderophores: classification, biosynthesis, perspectives of use in agriculture. Plants 2022;11(22). https://doi.org/10.3390/plants11223065.
[14] Meyer JM, Gruffaz C, Raharinosy V, Bezverbnaya I, Schäfer M, Budzikiewicz H. Siderotyping of fluorescent pseudomonas: molecular mass determination by mass spectrometry as a powerful pyoverdine siderotyping method. Biometals 2008;21(3):259–71. https://doi.org/10.1007/s10534-007-9115-6.
[15] Budzikiewicz H, Schäfer M, Fernández DU, Meyer JM. Structure proposal for a new pyoverdin from Pseudomonas sp PS 6.10. Z Naturforsch C Biosci 2006;61(11–12):815–20. https://doi.org/10.1515/znc-2006-11-1208.
[16] Visca P, Imperi F, Lamont IL. Pyoverdine siderophores: from biogenesis to biosignificance. Trends Microbiol 2007;15(1):22–30. https://doi.org/10.1016/j.tim.2006.11.004.
[17] Wei H, Aristilde L. Structural characterization of multiple pyoverdines secreted by two Pseudomonas strains using liquid chromatography-high resolution tandem

mass spectrometry with varying dissociation energies. Anal Bioanal Chem 2015; 407(16):4629–38. https://doi.org/10.1007/s00216-015-8659-5.
[18] Ruangviriyachai C, Fernández DU, Schäfer M, Budzikiewicz H. Structure proposal for a new pyoverdin from a Thai Pseudomonas putida strain1. Spectrosc Int J 2004; 18(3):453–8. https://doi.org/10.1155/2004/394872.
[19] Hannauer M, Schäfer M, Hoegy F, Gizzi P, Wehrung P, Mislin GLA, Budzikiewicz H, Schalk IJ. Biosynthesis of the pyoverdine siderophore of Pseudomonas aeruginosa involves precursors with a myristic or a myristoleic acid chain. Febs Lett 2012;586 (1):96–101. https://doi.org/10.1016/j.febslet.2011.12.004.
[20] Owen JG, Ackerley DF. Characterization of pyoverdine and achromobactin in Pseudomonas syringae pv. phaseolicola 1448a. BMC Microbiol 2011;11:218. https://doi.org/10.1186/1471-2180-11-218.
[21] Scholz K, Tiso T, Blank LM, Hayen H. Mass spectrometric characterization of siderophores produced by Pseudomonas taiwanensis VLB120 assisted by stable isotope labeling of nitrogen source. Biometals 2018;31(5):785–95. https://doi.org/10.1007/s10534-018-0122-6.
[22] Budzikiewicz H, Schäfer M, Meyer JM. Siderotyping of fluorescent Pseudomonas: gProblems in the determination of molecular masses by mass spectrometry. Mini-Rev Org Chem 2007;4(3):246–53. https://doi.org/10.2174/157019307781369968.
[23] Schalk IJ, Rigouin C, Godet J. An overview of siderophore biosynthesis among fluorescent Pseudomonads and new insights into their complex cellular organization. Environ Microbiol 2020;22(4):1447–66. https://doi.org/10.1111/1462-2920.14937.
[24] Fuchs R, Schafer M, Geoffroy V, Meyer JM. Siderotyping - a powerful tool for the characterization of pyoverdines. Curr Top Med Chem 2001;1(1):31–57. https://doi.org/10.2174/1568026013395542.
[25] Gu SH, Wei Z, Shao ZY, Friman VP, Cao KH, Yang TJ, Kramer J, Wang XF, Li M, Mei XL, Xu YC, Shen QR, Kümmerli R, Jousset A. Competition for iron drives phytopathogen control by natural rhizosphere microbiomes. Nat Microbiol 2020;5 (8):1002. https://doi.org/10.1038/s41564-020-0719-8.
[26] Ferret C, Cornu JY, Elhabiri M, Sterckeman T, Braud A, Jezequel K, Lollier M, Lebeau T, Schalk IJ, Geoffroy VA. Effect of pyoverdine supply on cadmium and nickel complexation and phytoavailability in hydroponics. Environ Sci Pollut Res 2015;22(3):2106–16. https://doi.org/10.1007/s11356-014-3487-2.
[27] David SR, Fritsch S, Forster A, Ihiawakrim D, Geoffroy VA. Flocking asbestos waste, an iron and magnesium source for. Sci Total Environ 2020;709:135936. https://doi.org/10.1016/j.scitotenv.2019.135936.
[28] David SR, Ihiawakrim D, Regis R, Geoffroy VA. Efficiency of pyoverdines in iron removal from flocking asbestos waste: an innovative bacterial bioremediation strategy. J Hazard Mater 2020;394:122532. https://doi.org/10.1016/j.jhazmat.2020.122532.
[29] Hazotte AA, Peron O, Abdelouas A, Montavon G, Lebeau T. Microbial mobilization of cesium from illite: the role of organic acids and siderophores. Chem Geol 2016; 428:8–14. https://doi.org/10.1016/j.chemgeo.2016.02.024.
[30] Nosrati R, Dehghani S, Karimi B, Yousefi M, Taghdisi SM, Abnous K, Alibolandi M, Ramezani M. Siderophore-based biosensors and nanosensors; new approach on the development of diagnostic systems. Biosens Bioelectron 2018;117:1–14. https://doi.org/10.1016/j.bios.2018.05.057.
[31] Yin K, Zhang WW, Chen LX. Pyoverdine secreted by Pseudomonas aeruginosa as a biological recognition element for the fluorescent detection of furazolidone. Biosens Bioelectron 2014;51:90–6. https://doi.org/10.1016/j.bios.2013.07.038.
[32] Budzikiewicz H, Schäfer M, Fernández DU, Matthijs S, Cornelis P. Characterization of the chromophores of pyoverdins and related siderophores by electrospray tandem mass spectrometry. Biometals 2007;20(2):135–44. https://doi.org/10.1007/s10534-006-9021-3.
[33] Georgias H, Taraz K, Budzikiewicz H, Geoffroy V, Meyer JM. The structure of the pyoverdin from Pseudomonas fluorescens 1.3.: structural and biological relationships of pyoverdins from different strains. Zeitschrift Fur Naturforschung C-a Journal of Biosciences 1999;54(5–6):301–8. https://doi.org/10.1515/znc-1999-5-602.
[34] Sultana R, Siddiqui BS, Taraz K, Budzikiewicz H, Meyer JM. A pyoverdine from Pseudomonas putida CFML 90-51 with a Lys ε-amino link in the peptide chain. Biometals 2000;13(2):147–52. https://doi.org/10.1023/A:1009212729408.
[35] Tappe R, Taraz K, Budzikiewicz H, Meyer JM, Lefevre JF. Structure elucidation of a pyoverdin produced by Pseudomonas-Aeruginosa Atcc-27853. J Prak Chem-Chem Ztg 1993;335(1):83–7. https://doi.org/10.1002/prac.19933350113.
[36] Weber M, Taraz K, Budzikiewicz H, Geoffroy V, Meyer JM. The structure of a pyoverdine from Pseudomonas sp. CFML 96.188 and its relation to other pyoverdines with a cyclic C-terminus. Biometals 2000;13(4):301–9. https://doi.org/10.1023/A:1009235421503.
[37] Pucciarelli S, Devaraj RR, Mancini A, Ballarini P, Castelli M, Schrallhammer M, Petroni G, Miceli C. Microbial consortium associated with the antarctic Marine ciliate euplotes focardii: an investigation from genomic sequences. Microb Ecol 2015;70(2):484–97. https://doi.org/10.1007/s00248-015-0568-9.
[38] Mozzicafreddo M, Pucciarelli S, Swart EC, Piersanti A, Emmerich C, Migliorelli G, Ballarini P, Miceli C. The macronuclear genome of the Antarctic psychrophilic marine ciliate Euplotes focardii reveals new insights on molecular cold adaptation. Sci Rep-Uk 2021;11(1):18782. https://doi.org/10.1038/s41598-021-98168-5.
[39] Ramasamy KP, Telatin A, Mozzicafreddo M, Miceli C, Pucciarelli S. Draft genome sequence of a new pseudomonas sp. Strain, ef1, associated with the psychrophilic antarctic ciliate. Microbiol Resour Ann 2019;8(41). https://doi.org/10.1128/MRA.00867-19.
[40] John MS, Nagoth JA, Ramasamy KP, Mancini A, Giuli G, Natalello A, Ballarini P, Miceli C, Pucciarelli S. Synthesis of bioactive silver nanoparticles by a pseudomonas strain associated with the antarctic psychrophilic Protozoon Euplotes focardii. Mar Drugs 2020;18(1):38. https://doi.org/10.3390/md18010038.
[41] Xiao R, Kisaalita WS. Purification of pyoverdines of Pseudomonas-Fluorescens-2-79 by copper-chelate chromatography. Appl Environ Microb 1995;61(11):3769–74. https://doi.org/10.1128/Aem.61.11.3769-3774.1995.
[42] Albrecht-Garry AM, Blanc S, Rochel N, Ocaktan AZ, Abdallah MA. Bacterial Iron transport - coordination properties of pyoverdin paa, a peptidic siderophore of Pseudomonas-Aeruginosa. Inorg Chem 1994;33(26):6391–402. https://doi.org/10.1021/ic00104a059.
[43] Boukhalfa H, Reilly SD, Michalczyk R, Iyer S, Neu MP. Iron(III) coordination properties of a pyoverdin siderophore produced by Pseudomonas putida ATCC 33015. Inorg Chem 2006;45(14):5607–16. https://doi.org/10.1021/ic060196p.
[44] Teintze M, Hossain MB, Barnes CL, Leong J, Van der Helm D. Structure of ferric pseudobactin: a siderophore from a plant growth promoting Pseudomonas. Biochemistry 1981;20(22):6446–57. https://doi.org/10.1021/bi00525a025.
[45] Budzikiewicz H, Kilz S, Taraz K, Meyer JM. Identical pyoverdines from Pesudomonas fluorescens 9AW and from Pseudomonas putida 9BW. Zeitschrift Fur Naturforschung C-a Journal of Biosciences 1997;52(11–12):721–8.
[46] Budzikiewicz H, Schröder H, Taraz K. Zur Biogenese der Pseudomonas-Siderophore: Der Nachweis analoger Strukturen eines Pyoverdin-Desferriferribactin-Paares [1]/The Biogenesis of Pseudomonas Siderophores: the Proof of Analogous Structures of a Pyoverdin/Desferriferribactin Pair [1], vol. 47; 1992. p. 26–32. https://doi.org/10.1515/znc-1992-1-206. 1-2.
[47] Jacques P, Ongena M, Gwose I, Seinsche D, Schroder H, Delfosse P, Thonart P, Taraz K, Budzikiewicz H. Structure and characterization of isopyoverdin from pseudomonas-putida Btp1 and its relation to the biogenetic pathway leading to pyoverdins. Z Naturforsch C Biosci 1995;50(9–10):622–9.